

Superradiant parametric X-ray emission

I. D. Feranchuk,^{1,*} N. Q. San,² and O. D. Skoromnik[†]

¹*Atomikus GmbH, Schoemperlen Str. 12a, 76185 Karlsruhe, Germany*

²*Department of Physics, Faculty of Electricity and Electronics, Nha Trang University, Nha Trang, Vietnam*

We compute a spectrum of parametric X-ray radiation (PXR) inside a crystal from a bunch of electrons, which is periodically modulated in density. We consider that the bunch of electrons is exiting from a XFEL channel. We demonstrate that in the case of a resonance between the frequency of parametric X-ray radiation and a frequency of modulation of an electron bunch the sequence of strong quasi-monochromatic X-ray pulses is formed — superradiant parametric X-ray emission (SPXE) with frequencies multiples of the modulation frequency. The number of photons in the impulse of SPXE in the case of an extremely asymmetric diffraction is comparable with the photon number in the impulse of a XFEL. Moreover the SPXE is directed under the large angle to the electron velocity and every harmonic in the spectrum is emitted under its own angle.

I. INTRODUCTION

Parametric X-ray radiation (PXR) is a well known mechanism of radiation from charged particles propagating in a periodic medium [1–8]. Its qualitative properties are the emission of quasi-monochromatic X-ray beams under the large angle to the electron velocity and the possibility to continuously tune the frequency of the radiation by simply rotating a crystal. As was firstly demonstrated in the work [9], when the electron density in the bunch reaches a critical value, the parametric beam instability can arise in analogy with the self amplified spontaneous emission (SASE) in the undulator of an XFEL. This process leads to a spatial modulation of an electron beam and the generation of a coherent X-ray radiation under the scale of the crystal length, which is much smaller than the typical XFEL undulator lengths. However, under the currently experimentally accessible electron-beams densities the length under which the parametric instability can be achieved is substantially larger than the X-ray absorption length in the crystal. Therefore, when an electron beam initially does not contain any modulation it is almost impossible to realize the SASE mechanism inside a crystal.

Before discussing the superradiant parametric X-ray emission (SPXE), let us briefly revise how the undulator is used in the XFEL case [10]. On the one hand due to the SASE mechanism the electron bunch, which density was initially uniformly distributed, is transformed into a sequence of micro-bunches that leads to the spatial modulation of the electron density with the period d_0 . This period is directly defined by the period of the undulator. Later when the bunch propagates inside the undulator the coherent radiation is formed (superradiant emission [10]) with the frequency $\omega_0 = 2\pi/d_0$; ($\hbar = c = 1$) and with the intensity proportional to the square of the number of electrons in the bunch. The coherent radiation is propagated in a small cone along the electron velocity.

The coincidence (resonance) between the modulation frequency of the bunch and the frequency of the emitted photons happens automatically since the beam modulation and the emission frequency are determined by the same undulator radiation mechanism.

Now let us consider the SPXE case when we suppose that an electron beam becomes modulated in density inside the undulator and in the end enters the crystalline target, where the PXR is generated with the frequency ω_B dependent on the crystal structure and the angle θ_B between the crystallographic planes and the electron velocity. As was recently demonstrated in the work [11] the highest intensity of PXR is reached when the electrons propagate in the grazing geometry, i.e., in a thin layer inside the crystal parallel to the crystal-vacuum interface and the X-ray photons are emitted under the large angle $2\theta_B$ to the electron velocity (PXR-EAD). The angle θ_B can be chosen in such a way that the resonant condition $\omega_0 \approx \omega_B$ is fulfilled. As a result, in addition to the main XFEL pulse a generation of SPXE will happen with the intensity also proportional to the square of the number of electrons in the bunch. According to Ref. [1] the spectral density of PXR photons emitted by a single electron can be larger than the corresponding density of the undulator radiation. Consequently, the number of SPXE photons can exceed the corresponding number of the XFEL ones. Besides, the SPXE photon pulse is directed under the large angle to the electron velocity, which enlarge the applicability of the XFEL by the creation of the additional exiting channels of X-rays. Fig. 1 presents the qualitative picture of processes which lead to the SPXE pulses in the XFEL channel.

In our work we describe a generation mechanism of SPXE and theoretically study characteristics of this new type of the coherent X-ray radiation.

II. QUALITATIVE ANALYSIS

We start the analysis of SPXE from its qualitative estimation by means of a simple and effective method of the description of electromagnetic processes of rela-

* Corresponding author: iferanchuk@gmail.com

† olegskor@gmail.com

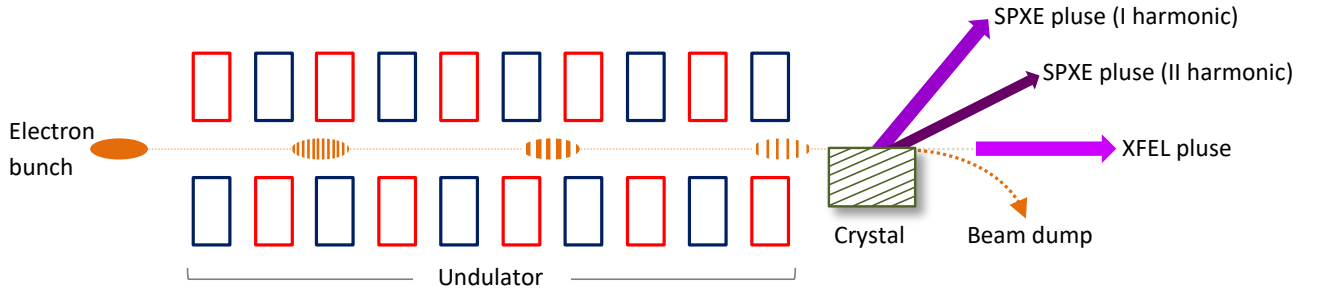


Figure 1. Qualitative scheme of the processes which lead to the generation of SPXE pulses in the XFEL channel

tivistic charged particles interacting with the medium, namely the method of equivalent photons (pseudo-photons, Weizsacker-Williams approximation) [12–14]. This approach is based on the observation that the self field of a relativistic charged particle is equivalent in its characteristics to the beam of pseudo-photons with a spectral-angular distribution $n(\mathbf{k})$ and a narrow angular divergence $\approx \gamma^{-1}$, which is determined by the relativistic gamma factor of the particle $\gamma = E/m$ [15]. As a result, the differential cross section $d\sigma_{if}^e$ of a transition $i \Rightarrow f$ between the initial i and final state f of a charged particle moving with a velocity \mathbf{v} and interacting with the medium is represented as

$$d\sigma_{if}^e = n(\mathbf{k})d\sigma_{if}^{\text{ph}}(\omega, \mathbf{k}_\perp)d\omega d\mathbf{k}_\perp, \quad (1)$$

where $d\sigma_{if}^{\text{ph}}$ is the cross section of the same transition for a photon with the frequency ω and the wave vector $\mathbf{k} = (\omega\mathbf{v}/v, \mathbf{k}_\perp)$.

In this framework PXR can be considered as a diffraction of a beam of pseudo-photons on the crystallographic planes. The spectral-angular distribution $n(\mathbf{k})$ of pseudo-photons for a single charged particle is well known [12–14] and is given by a smooth function of a frequency of the pseudo-photons. For relativistic particles the wave vector \mathbf{k} of a pseudo-photon can be approximated as $\mathbf{k} \approx \mathbf{k}_0 = \omega\mathbf{v}/v$ with $|\mathbf{k}_\perp| \ll k_0$. As a result, PXR peaks are determined by the frequencies ω_B when the wave vector \mathbf{k}_0 satisfies Bragg's condition. Consequently, the emitted photons are propagating in the directions of $\mathbf{k}_0 + \mathbf{g}$, where \mathbf{g} is one of the reciprocal lattice vectors of a crystal. As was demonstrated in Ref. [11] PXR will have the highest intensity when an electron moves in a crystal in a thin layer near to the crystal surface, EAD geometry, and the emitted radiation can exit the crystal without absorption, see Fig. 2.

When we now consider an electron bunch consisting of N electrons uniformly spread in space the total field will be given by an incoherent sum of fields from each electron. Therefore, the spectral-angular distribution of the pseudo-photons is simply defined by the sum of contributions from each particle and equals $Nn(\mathbf{k})$.

However, if the electron beam was moving through the undulator due to the SASE mechanism it became modulated. Accordingly its density becomes a periodic func-

tion of the longitudinal coordinate with the period d_0 . Consequently, this suggests that we might expect the coherent summation of individual fields from every electron. This results in the substantial modification of total spectral distribution of pseudo-photons in which we expect to see peaks with the amplitude proportional to the square of the number of particles in the beam. The frequencies of these spikes are harmonics of the frequency ω_0 . If the frequency of one of the peaks coincides with the frequency ω_B we should expect to see the resonant increase of the intensity of diffracted pseudo-photons. This corresponds exactly to the SPXE impulse. The SPXE emission happens when the Bragg's condition $2k_0d \sin \theta_B = 2\pi$ for the reflection of pseudo-photons from the crystallographic planes is simultaneously fulfilled with the coherence condition of the radiation from electrons of different micro-bunches $k_0d_0 = 2\pi$, that is

$$2d \sin \theta_B = d_0 \quad (2)$$

see Fig. 2.

Let us now investigate this process in more details. In the range of frequencies, which are much smaller than the particle energy E , i.e., $\omega \ll E$ the spectrum of pseudo-photons can be obtained via classical description [12]. The vector $\mathbf{A}(\mathbf{r}, t)$ and scalar $\varphi(\mathbf{r}, t)$ potentials from a beam of particles with charge e_0 that move uniformly in vacuum are defined by the Maxwell equations

$$\square \mathbf{A} = -4\pi e_0 \sum_a^N \mathbf{v}_a \delta(\mathbf{r} - \mathbf{v}_a t - \mathbf{r}_a), \quad (3)$$

$$\square \varphi = -4\pi e_0 \sum_a^N \delta(\mathbf{r} - \mathbf{v}_a t - \mathbf{r}_a), \quad (4)$$

where the sum runs over all particles and each particle is located at the initial position \mathbf{r}_a and has the velocity \mathbf{v}_a .

The Fourier transform of Eqs. (3-4) allows one to find the potentials and to calculate the electromagnetic fields.

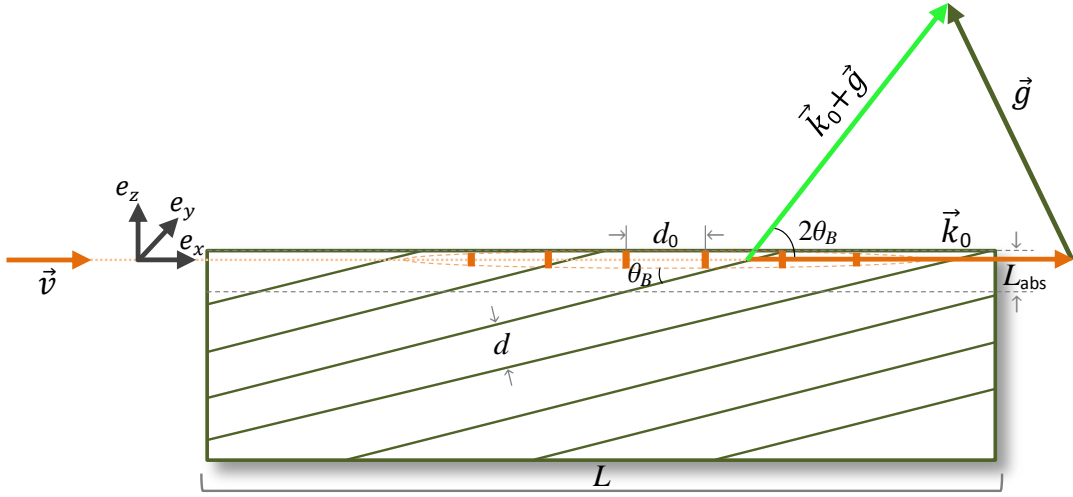


Figure 2. Scheme of the photon generation in the case of PXR-EAD geometry

$$\mathbf{E}(\mathbf{r}, t) = \sum_a^N \mathbf{E}_a(\mathbf{r}, t), \quad (5)$$

$$\mathbf{E}_a(\mathbf{r}, t) = -\frac{ie_0}{2\pi^2} \int d\mathbf{k} \frac{\mathbf{k} - \mathbf{v}_a(\mathbf{k}\mathbf{v}_a)}{k^2 - (\mathbf{k}\mathbf{v}_a)^2} e^{i\mathbf{k}(\mathbf{r} - \mathbf{v}_a t - \mathbf{r}_a)}, \quad (6)$$

$$\mathbf{H}(\mathbf{r}, t) = \sum_a^N \mathbf{v}_a \times \mathbf{E}_a(\mathbf{r}, t). \quad (7)$$

Now we estimate the fields in Eq. (5). For this we consider that the electron beam has a small angular divergence, such that the velocity of each particle can be presented as

$$\mathbf{v}_a = \mathbf{v} + \mathbf{v}'_a, \quad v'_a \ll v, \quad (8)$$

$$1 - v^2 = \frac{m^2}{E^2} \equiv \gamma^{-2} \ll 1. \quad (9)$$

We direct the x axis along the mean velocity \mathbf{v} of the bunch and suppose that the particle angular divergence is small with respect to this axis, i.e., $\theta_a < \gamma^{-1}$, where the angle θ_a defines this angular divergence. The fluctuations of the absolute value of the velocity are related to the nonmonochromaticity ΔE of the beam $|\mathbf{v}_a - \mathbf{v}| \approx \gamma^{-2} \Delta E/E \ll \gamma^{-2}$. Taking this into account we can represent the components of the fluctuation vector \mathbf{v}'_a of the

particle velocity with the accuracy up to γ^{-2} as

$$\mathbf{v}'_a = \theta_a - \frac{\theta_a^2}{2} \mathbf{e}_x, \quad \theta_a^2 = \theta_{az}^2 + \theta_{ay}^2, \quad (10)$$

$$\theta_a = \theta_{az} \mathbf{e}_z + \theta_{ay} \mathbf{e}_y, \quad (11)$$

where $\mathbf{e}_x, \mathbf{e}_y, \mathbf{e}_z$ are the unit vectors (see Fig. 2).

In this approximation the denominator of the field amplitude in Eq. (6) equals to

$$k_x^2 \gamma^{-2} + (\mathbf{k}_\perp - k_x \theta_a)^2, \quad (12)$$

and demonstrates that the main contribution to the field amplitude comes from the values

$$\theta_a \simeq \frac{k_\perp}{k_x} \simeq \gamma^{-1}. \quad (13)$$

For these angles the field up to accuracy γ^{-1} becomes transverse since $|E_x| \simeq \gamma^{-1} |E_\perp|$ and reads

$$\mathbf{E}_\perp(\mathbf{r}, t) = \sum_a^N \mathbf{E}_{a\perp}(\mathbf{r}, t), \quad (14)$$

$$\mathbf{E}_{a\perp}(\mathbf{r}, t) = -\frac{ie_0}{2\pi^2} \int d\mathbf{k} \frac{(\mathbf{k}_\perp - \theta_a k_x) e^{i\mathbf{k}(\mathbf{r} - \mathbf{v}_a t - \mathbf{r}_a)}}{k_x^2 \gamma^{-2} + (\mathbf{k}_\perp - k_x \theta_a)^2}, \quad (15)$$

$$\mathbf{H}(\mathbf{r}, t) = \mathbf{v} \times \mathbf{E}_\perp(\mathbf{r}, t).$$

The projection of the energy flux of the electromagnetic field on the x axis is determined by the following expression [12]

$$\begin{aligned} \Pi &= \frac{1}{4\pi} \int_{-\infty}^{\infty} dz dy dt [\mathbf{E}\mathbf{H}]_x = \int_{-\infty}^{\infty} dx dy dt |\mathbf{E}_\perp|^2 \approx \\ &\approx \frac{e_0^2}{2\pi^2 v} \sum_a \sum_b \int d\mathbf{k} \frac{(\mathbf{k}_\perp - \theta_a k_x)(\mathbf{k}_\perp - \theta_b k_x) e^{i\mathbf{k}(\mathbf{r}_b - \mathbf{r}_a)} e^{ix\mathbf{k}(\mathbf{v}'_a - \mathbf{v}'_b)}}{(k_x^2 \gamma^{-2} + (\mathbf{k}_\perp - k_x \theta_a)^2)(k_x^2 \gamma^{-2} + (\mathbf{k}_\perp - k_x \theta_b)^2)}, \end{aligned} \quad (16)$$

which can be split into the sum of two parts

$$\Pi = \Pi_{\text{sp}} + \Pi_{\text{coh}}. \quad (17)$$

The incoherent (spontaneous) flux Π_{sp} is given by the part of the sum when the summation indices coincide, i.e., $a = b$. After integration of this part over the variable $(\mathbf{k}_{\perp} - \boldsymbol{\theta}_a k_z) \Rightarrow \mathbf{k}_{\perp}$ the standard expression of the spectral density of pseudo-photons for the homogeneous electron beam is obtained [12]

$$\begin{aligned} \Pi_{\text{sp}} &= \frac{e_0^2}{v2\pi^2} N \int d\mathbf{k} \frac{k_{\perp}^2}{[k_x^2 \gamma^{-2} + \mathbf{k}_{\perp}^2]^2} = \int \omega n_{\text{sp}}(\omega) d\omega; \\ n_{\text{sp}}(\omega) &= N \frac{2e_0^2}{\pi\omega} \ln \frac{m\gamma}{\omega}, \end{aligned} \quad (18)$$

where $|\mathbf{k}_{\perp} - \boldsymbol{\theta}_a| \leq \omega\gamma^{-1}$ and N is the total number of electrons in the beam.

The coherent part is given via the following expression

$$\begin{aligned} \Pi_{\text{coh}} &= \frac{e_0^2}{2v\pi^2} \int d\mathbf{k} |\mathbf{F}(\mathbf{k})|^2, \\ \mathbf{F}(\mathbf{k}) &= \sum_a \frac{(\mathbf{k}_{\perp} - \boldsymbol{\theta}_a k_x)}{k_x^2 \gamma^{-2} + (\mathbf{k}_{\perp} - k_x \boldsymbol{\theta}_a)^2} e^{-i\mathbf{k}\mathbf{r}_a} e^{ix\mathbf{k}v'_a}, \end{aligned} \quad (19)$$

where $\mathbf{v}'_a = v\boldsymbol{\theta}_a$. To compute the form factor $\mathbf{F}(\mathbf{k})$ of the beam we need to average the obtained expression over the distribution on the coordinates \mathbf{r}_a and the angles $\boldsymbol{\theta}_a$ of the electrons in the beam. For this we can employ the theory of SASE mechanism of the XFEL, which yields the following expression for the desired distribution [10, 16]

$$\rho(\boldsymbol{\theta}) = \frac{1}{\pi\sigma_a^2} e^{-(\theta_z^2 + \theta_y^2)/\sigma_a^2}, \quad (20)$$

$$f(\mathbf{r}) = \frac{1}{\pi\sigma_b^2} e^{-(z^2 + y^2)/\sigma_b^2} \frac{1}{K} \sum_{l=0}^K \frac{1}{\sqrt{\pi}\sigma_c} e^{-(x - ld_0)^2/\sigma_c^2}. \quad (21)$$

Here the quantity σ_a defines the angular spread of the direction of the velocity, σ_b is the variance of the distribution over the transverse coordinates, d_0 is the period of the oscillations of the modulated bunch of length $L_b = Kd_0$. It is also assumed that the parameter σ_c that defines the fluctuations of the period of the oscillations $\sigma_c \ll d_0$ and the number of the micro-bunches $K \gg 1$. In addition, the distribution functions are normalized to unity.

Having this distribution, we can approximately substitute the summation over the discrete index a by the integration over the continuous variables

$$\sum_a \Rightarrow N \int d\mathbf{r} d\boldsymbol{\theta} f(\mathbf{r}) \rho(\boldsymbol{\theta}). \quad (22)$$

Let us now compute the integrals over the coordinates and angles. The coordinate part is simple and is given

via the Fourier transform of the Gaussian integral

$$\begin{aligned} \int d\mathbf{r} f(\mathbf{r}) e^{-i\mathbf{k}\mathbf{r}} &= e^{-(k_z^2 + k_y^2)\sigma_b^2/4} \frac{1}{K} \sum_{l=0}^K e^{-ik_x ld_0} e^{-k_x^2 \sigma_c^2/4} \\ &\approx e^{-(k_z^2 + k_y^2)\sigma_b^2/4} \frac{1 - e^{iL_b k_x}}{K(1 - e^{id_0 k_x})} e^{-k_x^2 \sigma_c^2/4}. \end{aligned} \quad (23)$$

The averaging over the angular spreads is reduced to the following integral

$$I = \int d\boldsymbol{\theta} \frac{e^{-\boldsymbol{\theta}^2/\sigma_a^2}}{k_x} \frac{1}{\pi\sigma_a^2} \frac{(\boldsymbol{\theta}_k - \boldsymbol{\theta}) e^{ixk_x v \boldsymbol{\theta}_k \cdot \boldsymbol{\theta}}}{(\gamma^{-2} + (\boldsymbol{\theta}_k - \boldsymbol{\theta})^2)}, \quad (24)$$

where $\boldsymbol{\theta}_k = \mathbf{k}_{\perp}/k$. To compute this integral, we first note that the characteristic angular spread of pseudo-photons is determined by the parameter $\theta_k \approx \gamma^{-1}$. Consequently, if the condition $\theta \approx \sigma_a \ll \gamma^{-1}$ is fulfilled we can ignore the influence of the angular spread of electron on the angular spread of pseudo-photons. This condition can be fulfilled for realistic emittances of electron beams [17]. As a result, in this approximation the desired integral is given by

$$I = \frac{1}{k_x} \frac{\boldsymbol{\theta}_k}{(\gamma^{-2} + \boldsymbol{\theta}_k^2)} e^{-(xkv)^2 \sigma_a^2 \boldsymbol{\theta}_k^2/4}. \quad (25)$$

As a result, we can find the expression for the coherent part Π_{coh} of the pseudo-photons flux

$$\begin{aligned} \Pi_{\text{coh}} &= \frac{N^2 e_0^2}{2v\pi^2} \int_0^\infty dk_x \int d\boldsymbol{\theta}_k \frac{\boldsymbol{\theta}_k^2 e^{-(xkv)^2 \sigma_a^2 \boldsymbol{\theta}_k^2/2 - \boldsymbol{\theta}_k^2 k^2 \sigma_b^2/2}}{(\gamma^{-2} + \boldsymbol{\theta}_k^2)^2} \\ &\times \left| \frac{1 - e^{iL_b k_x}}{K(1 - e^{id_0 k_x})} \right|^2 e^{-k_x^2 \sigma_c^2/2} \end{aligned} \quad (26)$$

We first evaluate the integral over the angles

$$J = \int d\boldsymbol{\theta}_k \frac{\boldsymbol{\theta}_k^2}{(\gamma^{-2} + \boldsymbol{\theta}_k^2)^2} e^{-a^2 \boldsymbol{\theta}_k^2}, \quad (27)$$

with $a^2 = 1/2[(xkv)^2 \sigma_a^2 + k^2 \sigma_b^2]$. The evaluation of this integral is done in the following way

$$\begin{aligned} J &= \pi \int_0^\infty du \frac{u}{(\gamma^{-2} + u)^2} e^{-a^2 u} \\ &= \pi \left[\int_0^\infty du \frac{e^{-a^2 u}}{(\gamma^{-2} + u)} - \int_0^\infty dx \frac{\gamma^{-2} e^{-a^2 u}}{(\gamma^{-2} + u)^2} \right] \\ &= \pi \left[-e^{a^2 \gamma^{-2}} \text{Ei}(-a^2 \gamma^{-2}) (1 + \gamma^{-2} a^2) - 1 \right]. \end{aligned} \quad (28)$$

In this equation $\text{Ei}(x)$ is the integral exponential function [18].

Thus the coherent part of the spectral density of the pseudo-photons is represented in the following way ($k_x = \omega/v$)

$$\begin{aligned} n_{\text{coh}}(\omega) &\approx \frac{N^2 e_0^2}{2\pi\omega v^2} \frac{d^2}{L_b^2} [-e^{a^2 \gamma^{-2}} \text{Ei}(-a^2 \gamma^{-2}) (1 + \gamma^{-2} a^2) - 1] \\ &\times \left| \frac{1 - e^{iL_b \omega/v}}{(1 - e^{id_0 \omega/v})} \right|^2 \exp[-\omega^2 \sigma_c^2/2]. \end{aligned} \quad (29)$$

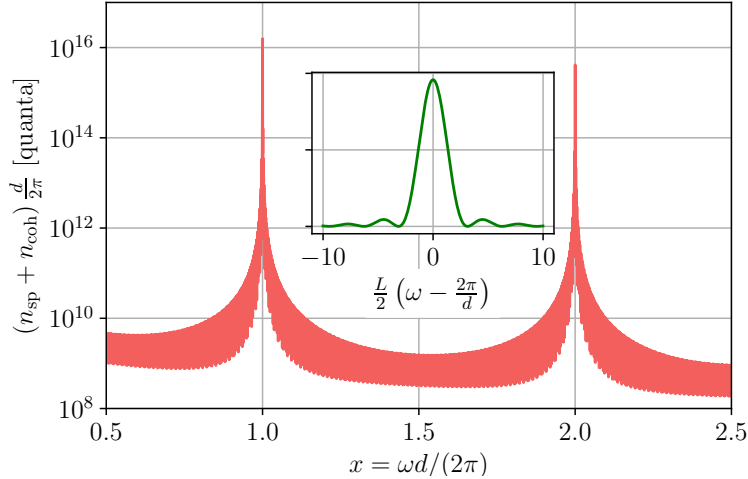


Figure 3. The incoherent and two harmonics of the coherent pseudo-photons spectral densities. The inset demonstrates the zoomed-in peak structure.

The spectral density $n_{\text{coh}}(\omega)$ of coherent pseudo-photons has sharp maximums when the frequency $\omega = 2\pi l/d$, $l = 1, 2, \dots$ and the result can be represented in the following form

$$n_{\text{coh}}(\omega) \approx \frac{N^2 e_0^2 d^2}{2\pi\omega v^2 L_b^2} [-e^{a^2\gamma^{-2}} \text{Ei}(-a^2\gamma^{-2})(1 + \gamma^{-2}a^2) - 1] \times \sum_l \frac{\sin^2[L_b(\omega - 2\pi l/d_0)/2v]}{\sin^2[d(\omega - 2\pi l/d)/2v]} e^{-2\pi^2 l^2 \sigma_c^2/d_0^2}. \quad (30)$$

The multiple $e^{-2\pi^2 \sigma_c^2/d^2} \leq 1$ as we supposed that fluctuation of the modulation period defined by the parameter $\sigma_c < d_0/2\pi$.

Let us compare the contributions from the coherent $n_{\text{coh}}(\omega)$ and incoherent $n_{\text{sp}}(\omega)$ parts of the spectral densities in Eq. (18). For this we choose the distribution of the pseudo-photons of the LCLS XFEL [17] facility. The typical electron energy is $E = 6.7$ GeV which corresponds to the electron gamma factor of $\gamma \approx 13111$. The parameters $\sigma_a = 10^{-4}$ and $\sigma_b = 2 \cdot 10^{-5}$ cm, parameter $a^2\gamma^{-2} \approx 0.2$. Let bunch the bunch charge be $Q = 0.2$ nC that corresponds to $N = 1.2 \cdot 10^9$ electrons. The duration of the photon pulse we can choose to be 25 fs, which corresponds to the modulated bunch length of $L_b = 8.3 \cdot 10^{-5}$ cm and the period of the modulation $d_0 = 10^{-8}$ cm with the parameter $\sigma_c = 10^{-8}$ cm. In Fig. 3 we plot the incoherent and two harmonics of the coherent spectral densities of the pseudo-photons of modulated beam with these parameters.

Finally, the typical frequency spread for the XFEL pulse $\Delta\omega/\omega \approx 10^{-3}$ and the frequency $\omega = 6.28 \cdot 10^8$ cm $^{-1}$. We can evaluate the number of the incoherent

pseudo-photons in this interval

$$N_{\text{sp}} = n_{\text{sp}}(\omega)\Delta\omega = N \frac{2e_0^2}{\pi} \frac{\Delta\omega}{\omega} \ln \frac{m\gamma}{\omega} = 1.1 \cdot 10^5. \quad (31)$$

This number is significantly smaller than the corresponding number of photons emitted by the XFEL pulse [17].

At the same time, the integration of the coherent distribution in the vicinity of the resonant frequency $\omega_l = 2\pi l/d_0$ can be fulfilled by means of the formula

$$\frac{\sin^2[L_b(\omega - 2\pi l/d_0)/2v]}{\sin^2[d(\omega - 2\pi l/d)/2v]} \approx 2\pi v \frac{L_b}{d^2} \delta(\omega - 2\pi l/d_0) \quad (32)$$

$L_b \gg d.$

It yields the number of pseudo-photons in the first harmonic, comparable with the number of photons in the XFEL pulse [17]

$$N_{\text{coh}} = \frac{N^2 e_0^2}{\omega_0 L_b} \left(\ln \frac{1}{a^2\gamma^{-2}} - C - 1 \right) \approx 5.9 \cdot 10^{11};$$

$$a^2\gamma^{-2} \ll 1. \quad (33)$$

Here $C \approx 0.577$ is the Euler constant. The number of pseudo-photons, corresponding to the second harmonic is ten times less.

As was discussed above, the reflection from the crystallographic planes leads to the conversion of the pseudo-photons into the real photons and corresponds to the SPXE process. The reflection coefficient of the pseudo-photons from the crystallographic planes is a function of the pseudo-photon frequency. Consequently, the intensity of the SPXE will reach its maximum when the maximum of the spectral density of the pseudo-photons coincides with the maximum of their reflection coefficient. If the position of a crystal is chosen as shown in Fig. 2

the pseudo-photons which wave vectors \mathbf{k} satisfy Bragg's condition with one of the reciprocal lattice vectors \mathbf{g} of the crystal will have maximal reflection coefficient, i.e.,

$$2\mathbf{k}_0 \cdot \mathbf{g} + \mathbf{g}^2 = 0, \quad (34)$$

where $\mathbf{k}_0 = \omega_0 \mathbf{v}/v$.

This means that the crystal should be oriented in such a way to the electron bunch that the angle between the electron velocity and the reflection plane equals

$$\theta_B = \arcsin \frac{g}{2\omega_0} \quad (35)$$

and the SPXE impulse will propagate in the direction of $\mathbf{k}_0 + \mathbf{g}$ under the angle $2\theta_B$ with respect to the electron velocity, see Fig. 2.

III. DYNAMIC THEORY OF SPXE

The analysis conducted in the previous sections is valid for the situation when the crystal is thin enough and the diffraction can be investigated in the framework of the kinematic theory. However, the intensity of SPXE reaches its maximum value when the electron propagates the distances in the crystal larger than the corresponding extinction length and consequently, the field created by the particles should be investigated in the framework of the dynamical diffraction theory [19].

This case for regular PXR was investigated in many works and the spectral-angular distribution of the emitted number of PXR quanta was obtained (see [1] and the references there in). The direct generalization of that results for the case of modulated beam leads to the following general expression for the spectral-angular distribution of the emitted number of quanta of SPXE photons

$$\begin{aligned} \frac{\partial^2 N_{n\omega s}}{\partial \omega \partial \Omega} &= \frac{\epsilon_0^2 \omega}{4\pi^2} \sum_a \sum_b \int \mathbf{E}_{\mathbf{k}s}^{(+)}(\mathbf{r}_a(t), \omega) \mathbf{v}_a e^{i\omega t} dt \\ &\times \int \mathbf{E}_{\mathbf{k}s}^{(+)*}(\mathbf{r}_b(t'), \omega) \mathbf{v}_b e^{-i\omega t'} dt', \quad (36) \\ \mathbf{r}_a(t) &= \mathbf{r}_a + \mathbf{v}_a t, \quad \mathbf{k} = -\mathbf{k}', \quad \mathbf{k}' = \omega \mathbf{n} \end{aligned}$$

where \mathbf{k}' is the wave vector of the photons emitted in the solid angle $d\Omega$, $\mathbf{E}_{\mathbf{k}s}^{(+)}(\mathbf{r}, \omega)$ is the solution of the Maxwell equations, which describes the diffraction of the plane wave $\mathbf{e}_s e^{i\mathbf{k} \cdot \mathbf{r}}$ with the polarization \mathbf{e}_s on the crystal and possesses the asymptotic of the plane wave and an outgoing spherical wave. The use of the wave vector $\mathbf{k} = -\mathbf{k}'$ and the field $\mathbf{E}_{\mathbf{k}s}^{(+)}$ is related to the fact that for the radiation exited from the crystal one should exploit the reciprocity theorem of optics [20] that relates the waves with different asymptotics, i.e., $\mathbf{E}_{\mathbf{k}s}^{(+)} = \mathbf{E}_{-\mathbf{k}s}^{(-)*}$. In addition, it was recently demonstrated that the intensity of the PXR reaches maximal values in the so called grazing geometry when the extremely asymmetric diffraction happens. In this case the electrons move along the crystal surface inside the crystal and the vector $\mathbf{k}_g = \mathbf{k} + \mathbf{g}$

is anti-parallel to the electron velocity, i.e. $\mathbf{k}_g \parallel (-\mathbf{v})$ (see Fig. 4).

To find the field created by the particle inside a crystal we can use the results from the Ref. [21] where a two-wave approximation [1, 19] of the dynamical diffraction theory was employed according to which the field within the crystal is expressed as

$$\mathbf{E}_{\mathbf{k}s}^{(+)}(\mathbf{r}, \omega) = \mathbf{e}_s E_{\mathbf{k}s} e^{i\mathbf{k} \cdot \mathbf{r}} + \mathbf{e}_{1s} E_{\mathbf{k}_g s} e^{i\mathbf{k}_g \cdot \mathbf{r}}, \quad (37)$$

$$\mathbf{k}_g = \mathbf{k} + \mathbf{g}. \quad (38)$$

Here \mathbf{e}_s and \mathbf{e}_{1s} ($s = 1, 2$) are the polarization vectors of the incident and the diffracted waves Fig. 4. Their amplitudes satisfy the algebraic system of homogeneous equations

$$\begin{aligned} \left(\frac{k^2}{k_0^2} - 1 - \chi_0 \right) E_{\mathbf{k}s} - c_s \chi_{-\mathbf{g}} E_{\mathbf{k}_g s} &= 0, \\ \left(\frac{k_g^2}{k_0^2} - 1 - \chi_0 \right) E_{\mathbf{k}_g s} - c_s \chi_{\mathbf{g}} E_{\mathbf{k}s} &= 0; \end{aligned} \quad (39)$$

where $k_0 = \omega$, χ_0 and $\chi_{\mathbf{g}}$ are the Fourier components of the crystal susceptibility $\chi(\mathbf{r})$

$$\chi(\mathbf{r}) = \sum_{\mathbf{g}} \chi_{\mathbf{g}} e^{i\mathbf{g} \cdot \mathbf{r}}. \quad (40)$$

The coefficient $c_s = 1$ for the σ polarization ($s = 1$) and $c_s = \cos 2\theta_B$ for the π polarization ($s = 2$) of the incident and diffracted waves respectively. In addition, we note that the waves of different polarizations propagate independently if we neglect terms of the order of $\sim |\chi_0|^2$ in the Maxwell equations [11, 19, 22].

The field amplitudes in vacuum and in crystal should satisfy the boundary conditions on the crystal-vacuum interface such that the total field intensity is continuous. Additionally, one needs to take into account in vacuum not only an incident wave, but also a specularly reflected diffracted wave $\mathbf{E}_{\mathbf{k}_g s}^{(sp)} = \mathbf{e}_{1s} E_{\mathbf{k}_g s}^{(sp)} \exp[i(\mathbf{k}_{\parallel} + \mathbf{g}_{\parallel}) \cdot \mathbf{r} + ik'_{gz} z]$, $k'_{gz} = \sqrt{k_0^2 - (\mathbf{k}_{\parallel} + \mathbf{g}_{\parallel})^2}$, where \mathbf{k}_{\parallel} and \mathbf{g}_{\parallel} are the projections of the vectors on the crystal surface. As a result the following expressions for the field inside and outside the crystal were found [21]

$$\mathbf{E}_{\mathbf{k}s}^{(+)} = \mathbf{e}_s e^{i\mathbf{k} \cdot \mathbf{r}} + \mathbf{e}_{1s} E_s^{(sp)} e^{i(\mathbf{k}_{\parallel} + \mathbf{g}_{\parallel}) \cdot \mathbf{r}} e^{ik'_{gz} z}, \quad z > 0, \quad (41)$$

$$\mathbf{E}_{\mathbf{k}s}^{(+)} = e^{i\mathbf{k} \cdot \mathbf{r}} \sum_{\mu=1,2} e^{-ik_0 z \epsilon_{\mu s}} (\mathbf{e}_s E_{\mu s} + \mathbf{e}_{1s} E_{g\mu s} e^{i\mathbf{g} \cdot \mathbf{r}}), \quad z < 0, \quad (42)$$

where the x axis is directed along the propagation direction of the electron bunch and the z axis is directed perpendicular to crystal surface. The coordinate x is changing in the limits $0 < x < L$, with L being the crystal length, Fig. 2 and the point $z = 0$ denotes the crystal surface with $z < 0$ is the crystal and $z > 0$ is vacuum. The quantities $\epsilon_{\mu s}$ define the wave vector inside the crystal and are determined from the condition

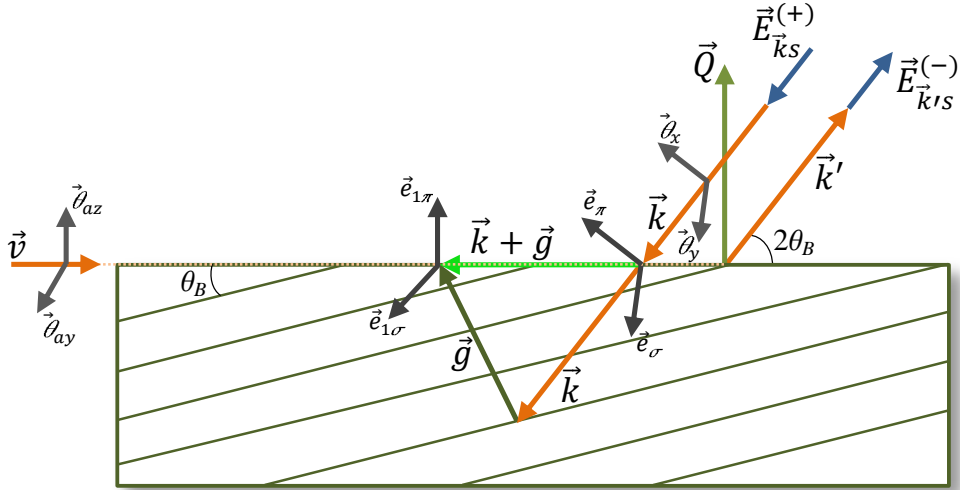


Figure 4. The geometry for the dynamical diffraction theory of SPXE

that the system of homogeneous equations (39) has a nontrivial solution. The \mathbf{Q} is the normal to the crystal surface. The field amplitudes $E_s^{(sp)}$, $E_{\mu s}$ and $E_{g\mu s}$ are found from the boundary conditions. According to the boundary conditions the in-plane component \mathbf{k}_{\parallel} of the wave vector is conserved. Finally, it was found that the main contribution to the number of emitted photons is given by the amplitude E_{g1s} which reads

$$E_{g1s} = \frac{c_s \chi_g}{\alpha_B + \chi_0}, \quad (43)$$

$$\alpha_B = \frac{(\mathbf{k} + \mathbf{g})^2 - k_0^2}{k_0^2}. \quad (44)$$

Here the coefficient α_B defines the deviation from the Bragg's condition.

As in the case of kinematic theory we can split the total intensity in Eq. (36) into the coherent and incoherent parts. The latter part corresponds to the situation when in the double sum we select only the terms with identical indices, i.e., $a = b$. This contribution is proportional to the number of electrons in the bunch N and corresponds to the spontaneous parametric X-ray radiation (PXR):

$$\frac{\partial^2 N_{\mathbf{n}\omega s}^{\text{SP}}}{\partial \omega \partial \Omega} = N \frac{e_0^2 \omega}{4\pi^2} \left| \int \mathbf{E}_{\mathbf{k}s}^{(+)}(\mathbf{r}(t), \omega) \mathbf{v} e^{i\omega t} dt \right|^2, \quad (45)$$

$$\mathbf{r}(t) = \mathbf{r}_0 + \mathbf{v}t.$$

The integral over the electron trajectory was computed in Ref. [21], which yields the

$$\frac{\partial^2 N_{\mathbf{n}\omega s}^{\text{SP}}}{\partial \theta_x \partial \theta_y} = N \frac{e_0^2}{4\pi \hbar c} \frac{[(\theta_y - \theta_{ay})^2 + (\theta_x - \theta_{ax})^2 \cos^2 2\theta_B] |\chi_g|^2}{[\gamma^{-2} + (\theta_y - \theta_{ay})^2 + (\theta_x - \theta_{ax})^2 - \chi_0^2]^2} \times \frac{(1 - e^{-Lk_0 \chi_0'' |\theta_{az}|})}{\chi_0'' |\theta_{az}|} e^{-\chi_0'' k_0 |z_0|}. \quad (46)$$

In this equation the angles θ_a, θ - angular variables of the electron and the emitted photon correspondingly (

Fig. 4). They define the small deviations of the electron velocity the photon wave vector from the ideal values that is

$$\mathbf{v}_a = v \left(1 - \frac{\theta_a^2}{2}\right) \mathbf{e}_x + \boldsymbol{\theta}_a; \quad (\mathbf{e}_x \boldsymbol{\theta}_a) = 0;$$

$$\mathbf{k} = k_0 \left(1 - \frac{\theta_a^2}{2}\right) + k_0 \boldsymbol{\theta}; \quad (\mathbf{k}_0 \boldsymbol{\theta}) = 0;$$

$$\omega + (\mathbf{k}_0 + \mathbf{g}) \cdot \mathbf{v} = 0; \quad 2(\mathbf{k}_0 \mathbf{g}) + g^2 = 0. \quad (47)$$

The integral over $\boldsymbol{\theta}$ and averaging over the electron angles was computed in Ref. [21]. As for example, for Si crystal the characteristic value of the photon number for PXR in EAD geometry is

$$N_{\text{PXR}}^{\text{SP}} \approx 2.2 \cdot 10^{-5} \times N \approx 0.3 \cdot 10^5, \quad (48)$$

for the bunch with charge $Q_0 = 0.2$ nC, i.e. $N = 1.3 \cdot 10^9$.

This value is comparable with the value of spontaneous pseudo-photons defined by Eq. (31) that is the crystal is working as the reflective mirror for this interval of the pseudo-photon spectrum.

Now let us come back to compute the coherent part of the distribution. If we perform the same substitution from the summation over the discrete index by the integration over the electron distribution. In this case the calculation is reduced to the calculation of the following averaging with the distribution functions of the bunch

$$\frac{\partial^2 N_{\mathbf{n},\omega s}^{\text{coh}}}{\partial \omega \partial \Omega} = N^2 \frac{e_0^2 \omega}{4\pi^2} |F_s(\mathbf{k})|^2 \quad (49)$$

$$F_s(\mathbf{k}) = \frac{1}{N} \int \langle \sum_a \mathbf{E}_{\mathbf{k}s}^{(+)}(\mathbf{r}_a(t), \omega) \mathbf{v}_a e^{i\omega t} \rangle dt, \quad (50)$$

$$\mathbf{v}_a = \mathbf{v} \left(1 - \frac{\theta_a^2}{2}\right) + v \boldsymbol{\theta}_a, \quad \mathbf{v} \cdot \boldsymbol{\theta}_a = 0. \quad (51)$$

Here we considered that the electron velocity has deviations from the x axis and these deviations are described

by the $\boldsymbol{\theta}_a$. The vector \mathbf{v} is the mean velocity of the electron bunch and is directed along the x axis (Fig. 4).

As was already discussed the SPXE emission is related to the motion of the bunch of electrons in a thin layer inside the crystal parallel to the crystal vacuum interface. In this case the electron velocity is perpendicular to the normal \mathbf{Q} to the crystal surface, i.e., $\mathbf{v} \cdot \mathbf{Q} = 0$. We are interested in the diffracted wave, that is the wave which is propagating in the direction $\mathbf{k}_g = \mathbf{k} + \mathbf{g}$. Consequently, the main contribution is given by the E_{g1s} amplitude. Therefore the field which is entering into the desired averaging reads

$$\begin{aligned} \mathbf{E}_{\mathbf{k}s}^{(+)}(\mathbf{r}_a(t), \omega) e^{i\omega t} &= \mathbf{e}_{1s} E_{g1s} \\ &\times \exp\{i(\omega + \mathbf{k}_g \cdot \mathbf{v} - \omega \mathbf{Q} \cdot \boldsymbol{\theta}_{\epsilon_{1s}})t \\ &\quad + i\mathbf{v} \mathbf{k}_g \cdot \boldsymbol{\theta}_a t - i\mathbf{k}_g \cdot \mathbf{v} t \theta_a^2 / 2 \\ &\quad + i\mathbf{k}_g \cdot \mathbf{r}_a - i\mathbf{k}_0 \mathbf{r}_a \cdot \mathbf{Q} \epsilon_{1s}\}. \end{aligned} \quad (52)$$

According to the results of Ref. [21] the SPXE peak is located near the direction defined by the conditions

- Bragg's diffraction condition

$$\alpha_B = \frac{(\mathbf{k} + \mathbf{g})^2 - k_0^2}{k_0^2} = 0. \quad (53)$$

- The Cherenkov radiation condition

$$(\mathbf{k} + \mathbf{g}) \cdot \mathbf{v} = -k_0 = -\omega. \quad (54)$$

- The condition that extremely asymmetric diffraction happens, i.e. the diffracted wave is propagating in the direction of \mathbf{k}_g , which lies in the crystal plane defined by the normal to the crystal surface \mathbf{Q}

$$(\mathbf{k} + \mathbf{g}) \cdot \mathbf{Q} = 0. \quad (55)$$

Taking into account these considerations we can represent the vector \mathbf{k}_g in the following way

$$\mathbf{k}_g = -\frac{\omega}{v^2} \mathbf{v} \left(1 - \frac{\theta^2}{2}\right) + \omega \boldsymbol{\theta}, \quad \boldsymbol{\theta} \cdot \mathbf{v} = 0, \quad (56)$$

With this the form factor of the bunch is defined by the following integral with the accuracy $\sim \theta^3$

$$\begin{aligned} F_s(\omega, \boldsymbol{\theta}) &= \int_0^L dt \mathbf{e}_{1s} \cdot \mathbf{v} \frac{c_s \chi_g}{\alpha_B + \chi_0} e^{i(\omega + \mathbf{k}_g \cdot \mathbf{v} - \omega \mathbf{Q} \cdot \boldsymbol{\theta}_{\epsilon_{1s}})t} J, \\ J &= \int d\mathbf{r}_a d\boldsymbol{\theta}_a f(\mathbf{r}_a) \rho(\boldsymbol{\theta}_a) \exp\{i\omega \boldsymbol{\theta}_a t + \frac{i\omega t \theta_a^2}{2} \\ &\quad + i\omega(-x_a + \boldsymbol{\theta} \mathbf{r}_a)\} \end{aligned} \quad (57)$$

The evaluation of the integral J over electron angle and coordinates with the Gaussian distribution Eqs. (20)-(21) yields

$$\begin{aligned} J &= \exp\left\{-\frac{\omega^2 t^2 \theta^2 \sigma_a^2}{4(1 + i\omega t \sigma_a^2)} - \frac{\omega^2 \theta^2 \sigma_b^2}{4} - \frac{\omega^2 \sigma_c^2}{4}\right\} \\ &\times \frac{1 - e^{iL_b \omega}}{K(1 - e^{id_0 \omega})}. \end{aligned} \quad (58)$$

The maxima of J as a function of ω are located on the frequencies ω of the radiation, which are proportional to the frequencies of the modulation of the electron beam, i.e., $\omega = \omega_0 n$, where $\omega_0 = 2\pi/d_0$. In addition, it follows from Eq. (58) that the major contribution to the coherent impulse of SPXE comes from the part of an electron trajectory and scattering angles for which the following conditions are fulfilled

$$\omega t \theta \sigma_a < 1, \quad (59)$$

$$\omega \theta \sigma_b < 1. \quad (60)$$

Since the angular spread σ_a of ultra-relativistic electrons in the beam of XFEL is significantly smaller than the angular spread of PXR photons, for which $\theta \simeq \sqrt{|\chi'_0|}$ [1] the terms $\omega t \sigma_a^2$ in Eq. (58) can be neglected. In this case one can perform the integration over time t in analytical form. This gives

$$\begin{aligned} F_s(\omega, \boldsymbol{\theta}) &= \frac{c_s(\mathbf{e}_{1s} \cdot \mathbf{v}) \chi_g}{\alpha_B + \chi_0} \frac{1 - e^{iL_b \omega}}{K(1 - e^{id_0 \omega})} \\ &\times e^{-\frac{\omega^2 \sigma_c^2}{4} - \frac{\omega^2 \theta^2 \sigma_b^2}{4}} e^{-\frac{q_s^2}{\delta^2} \frac{\sqrt{\pi}}{\delta}} \\ &\times \left[\Phi\left(\frac{L\delta}{2} + i\frac{q_s}{\delta}\right) - \Phi\left(-i\frac{q_s}{\delta}\right) \right], \end{aligned} \quad (61)$$

where $\Phi(x) = \frac{2}{\sqrt{\pi}} \int_x^\infty e^{-y^2} dy$ is the complementary error function, $\delta = \omega \theta \sigma_a$, $q_s = \omega + \mathbf{k}_g \cdot \mathbf{v} - \omega \mathbf{Q} \cdot \boldsymbol{\theta}_{\epsilon_{1s}}$ and L_b is the length of the electron pulse.

According to Ref. [21] when Eqs. (55-54) and the additional condition $\theta \gg \sigma_a$ are satisfied the quantity α_B is expressed through the angular variables of a photon as

$$\alpha_B \approx -(\gamma^{-2} + \theta^2). \quad (62)$$

As a result, we obtain an expression for the spectral-angular distribution of photons in the coherent part of SPXE pulse, which for the first harmonic $u = \omega - 2\pi/d_0$

$$\begin{aligned} \frac{\partial^2 N_{\mathbf{n}\omega s}^{\text{coh}}}{\partial \omega \partial \Omega} &= N^2 \frac{e_0^2 \omega}{4\pi^2} \frac{c_s^2 (\mathbf{e}_{1s} \cdot \mathbf{v})^2 |\chi_g|^2}{(\gamma^{-2} + \theta^2 - \chi'_0)^2} \frac{\sin^2 L_b u / 2}{K^2 \sin^2 d_0 u / 2} \\ &\times \exp\left\{-\frac{2\pi^2 \sigma_c^2}{d^2} - \frac{\omega^2 \theta^2 \sigma_b^2}{2} - 2\frac{q_s^2}{\delta^2}\right\} \\ &\times \frac{\pi}{\delta^2} \left| \Phi\left(\frac{L\delta}{2} - i\frac{q_s}{\delta}\right) - \Phi\left(-i\frac{q_s}{\delta}\right) \right|^2. \end{aligned} \quad (63)$$

Now we compute the total number of quanta in the coherent part of SPXE. For this we need to integrate the spectral-angular distribution (63) over the angles and frequencies. To compute the integral over the frequencies we make use of the following relation

$$\frac{\sin^2 L_b u / 2}{K^2 \sin^2 d_0 u / 2} \approx 2\pi \frac{1}{L_b} \delta(\omega - \omega_0), \quad (64)$$

which is valid when $K = L_b/d_0 \gg 1$. Here $\omega_0 = 2\pi/d_0$. Consequently, the integration over the frequency becomes

trivial

$$\begin{aligned} \frac{\partial^2 N_{\mathbf{n}\omega s}^{\text{coh}}}{\partial \Omega} &= N^2 \frac{e_0^2 \omega}{2L_b} \frac{c_s^2 (\mathbf{e}_{1s} \cdot \mathbf{v})^2 |\chi_g|^2}{(\tilde{\gamma}^{-2} + \theta^2 - \chi_0')^2} \\ &\times \exp \left\{ -\frac{2\pi^2 \sigma_c^2}{d^2} - \frac{\omega^2 \theta^2 \sigma_b^2}{2} - 2\frac{q_s^2}{\delta^2} \right\} \\ &\times \frac{1}{\delta^2} \left| \Phi \left(\frac{L\delta}{2} - i\frac{q_s}{\delta} \right) - \Phi \left(-i\frac{q_s}{\delta} \right) \right|^2. \end{aligned} \quad (65)$$

When an electron bunch moves in the crystal its angular divergence increases due to the multiple scattering on the atoms of the crystal. As was demonstrated in Ref. [23] for PXR from ultrarelativistic electrons, it can be taken into account with the help of the substitution

$$\begin{aligned} \gamma^{-2} &\Rightarrow \tilde{\gamma}^{-2} = \gamma^{-2} + \theta_s^2, \\ \theta_s^2 &= \left(\frac{E_s}{E} \right)^2 \frac{L}{L_R}, \end{aligned} \quad (66)$$

where L_R is the radiation length [13] and $E_s \approx 21$ MeV.

Let us now investigate this expression for the case of an ideal electron beam for which the following conditions are fulfilled

$$\frac{2\pi^2 \sigma_c^2}{d_0^2} < 1, \quad (67)$$

$$\omega^2 \theta^2 \sigma_b^2 \approx \omega^2 |\tilde{\gamma}^{-2} - \chi_0'| \sigma_b^2, \quad (68)$$

$$\delta^2 L^2 = (\omega \theta \sigma_a)^2 L^2 \approx (\omega L \sigma_a)^2 |\tilde{\gamma}^{-2} - \chi_0'| < 1. \quad (69)$$

The first condition means that the fluctuations of the modulation period are rather small. The meaning of the remaining ones is that the relative transverse width and the angular spread of the particles in the bunch are less than the angular divergence of the photons in the PXR pulse [21]. These conditions restrict the exploited electron beams only to the high quality ones with a low emittance. For example, if we consider electrons with the energy of 14 GeV, propagating through a silicon crystal of a thickness $L = 1$ cm and generating photons with the energy of 10 KeV ($|\chi_0'| \approx 10^{-5}$), then we get the following estimation for the beam emittance

$$\begin{aligned} \sigma_b^2 &< 10^{-11} \text{ cm}, \sigma_a^2 < 10^{-9} \text{ rad}, \\ \epsilon &= \sigma_b \sigma_a < 10^{-10} \text{ cm} \times \text{rad}, \end{aligned} \quad (70)$$

which is sizable for the LCLS facility.

Under the assumptions of Eqs. (67-69) we can further simplify the expression for the number of emitted photons. For this we notice that for large x the complementary error function can be replaced by its asymptotic representation $\Phi(x) \approx 1/\sqrt{\pi} e^{-x^2}/x$ and Eq. (65) is further simplified

$$\begin{aligned} \frac{\partial N_{\mathbf{n}s}^{\text{coh}}}{\partial \Omega} &= N^2 \frac{e_0^2 \omega_0}{2L_b} \frac{c_s^2 (\mathbf{e}_{1s} \cdot \mathbf{v})^2 |\chi_g|^2}{(\tilde{\gamma}^{-2} + \theta^2 - \chi_0')^2} \\ &\times \frac{1}{\pi} \left| \frac{1 - e^{iq_s L}}{q_s} \right|^2. \end{aligned} \quad (71)$$

Now taking into account that when $\omega L \gg 1$ we replace [1]

$$\frac{1}{\pi} \left| \frac{1 - e^{iq_s L}}{q_s} \right|^2 = \frac{4 \sin^2 L q_s / 2}{\pi q_s^2} \approx 2L \delta(q_s) \quad (72)$$

and integrate over the angle θ_x in the plane, defined by the vectors \mathbf{v} and \mathbf{g} with the value

$$\begin{aligned} q_s &= \omega_0 + (\mathbf{k}_g \mathbf{v}) - \omega_0 \epsilon_{1s} \theta_x \\ &\approx \omega_0 + (\mathbf{k}_0 + \mathbf{g}) \cdot \mathbf{v} - \omega_0 \theta_x \sin 2\theta_B = 0; \\ \theta_x &= \frac{(\mathbf{k}_0 + \mathbf{g}) \cdot \mathbf{v}}{\omega_0 \sin 2\theta_B} = 0. \end{aligned} \quad (73)$$

As a result, the photons are emitted with the polarization proportional to θ_y and directed along the vector $\mathbf{v} \times \mathbf{g}$ (Fig. 4). Thus we get

$$\frac{\partial N_{\theta_y}^{\text{coh}}}{\partial \theta_y} = N^2 \frac{e_0^2 |\chi_g|^2 \theta_y^2}{(\tilde{\gamma}^{-2} + \theta_y^2 - \chi_0')^2} \frac{L}{L_b \sin 2\theta_B}. \quad (74)$$

Finally, after the integration over the remaining angle θ_y one obtains the total number of the SPXE photons:

$$N_{\text{SPXE}} = N^2 \frac{e_0^2 |\chi_g|^2 \pi}{2\sqrt{\tilde{\gamma}^{-2} - \chi_0'}} \frac{L}{L_b \sin 2\theta_B}. \quad (75)$$

This result provides a clear qualitative interpretation if we relate N_{SPXE} with the number of the coherent pseudo-photons N_{coh} , defined by Eq. (33). With the logarithmic accuracy one obtains

$$N_{\text{SPXE}} \approx \frac{\pi}{2 \sin 2\theta_B} \frac{|\chi_g|^2 \omega_0 L}{\sqrt{\tilde{\gamma}^{-2} - \chi_0'}} N_{\text{coh}}. \quad (76)$$

The refraction coefficient R of X-ray radiation on the crystallographic planes is defined by the equation [22]

$$R \approx |\chi_g|^2 (\omega_0 L)^2$$

Here the Bragg's condition is fulfilled.

If one takes into account the ratio of the angular width of the Bragg's peak $\Delta\theta_B \approx (\omega_0 L)^{-1}$ to the angular spread of the pseudo-photons $\Delta\theta_{\text{ps}} \approx \sqrt{\tilde{\gamma}^{-2} - \chi_0'}$ then Eq. (76) takes the following form

$$N_{\text{SPXE}} \approx \frac{\pi}{2 \sin 2\theta_B} R \frac{\Delta\theta_B}{\Delta\theta_{\text{ps}}} N_{\text{coh}}. \quad (77)$$

This relation demonstrates that the SPXE emerges as a result of the reflection of coherent pseudo-photons from the crystallographic planes. The frequencies of these pseudo-photons are located near the frequency of the resonance $\omega_0 = 2\pi/d_0$.

The real photons are emitted under the large angle $2\theta_B$ to the electron velocity. Thus, by choosing orientation of the crystal the photons can be directed in any desired location. This allows one to obtain additional experimental windows in the XFEL experiments.

In order to get a quantitative estimation we consider that an electron bunch has a charge of 0.2 nC and the length $L_b = 8.3 \cdot 10^{-5}$ cm.

For the crystal parameters we will employ the values taken from the X-ray database [24] for the SPXE radiation generated in a Si crystal by the reflection (400) and $\theta_B = \pi/4$

$$\begin{aligned} \hbar\omega_B &= 6.45 \text{ keV}; k_0 = 3.27 \cdot 10^8 \text{ cm}^{-1}; \\ E &= 6.7 \text{ GeV}; |\chi_g| = 0.12 \cdot 10^{-4}; \chi'_0 = -0.24 \cdot 10^{-5}; \\ L &= 1.0 \text{ cm}; \tilde{\gamma}^{-2} = 7.5 \cdot 10^{-7} \end{aligned} \quad (78)$$

The crystal surface is defined by the plane $\langle 110 \rangle$. The photons will be emitted under the angle $\pi/2$ to the electron velocity.

As a result, we obtain the number of photons in the coherent part of SPXE

$$N_{\text{SPXE}} \approx 5.7 \cdot 10^{12} \text{ quanta} \quad (79)$$

with the angular spread $\delta\theta$ and spectral width $\Delta\omega/\omega$ of the order $\sqrt{\tilde{\gamma}^{-2} - \chi'_0} \approx 0.51 \times 10^{-3}$, which are comparable with the XFEL values.

Also we pay attention to the fact that according to Eq. (2) the higher harmonics of SPXE will be generated (for the harmonic n the condition $\pi n \sigma_c < d$ should be satisfied). Moreover they all will be directed under different angles with respect to the electron velocity. For example, for the same crystal parameters the photons with energy $\hbar\omega_B = 12.9$ keV will be generated under the angle 40.5° to the electron velocity. This allows one to

obtain also intensive pulses of the harder X-rays without the need to change the electron energy that is not possible for XFEL.

IV. CONCLUSIONS

In the present paper a new application of the modulated electron bunches is considered. It is supposed that such bunches are formed in the XFEL undulator due to SASE mechanism and it is shown that the spectrum of the self electromagnetic field (pseudo-photon spectrum) of such bunches is essentially transforms and includes intense peaks at the frequencies proportional to the modulation frequency. When such bunch goes through the crystal disposed at the undulator exit the superradiant parametric X-ray emission (SPXE) is generated. Electrons move in the thin layer along the crystal surface and generate X-ray pulse that is emitted at the large angle to the direction of the electron velocity. Intensity of this pulse is proportional to the square of the number of electrons in the bunch and its characteristics are comparable with the parameter of the main XFEL pulse, which is directed along the electron velocity. SPXE pulses can be used for creation of additional windows for XFEL. Moreover the higher harmonics of SPXE can be used for generation of the pulses of harder X-rays and they do not require to change the energy of the electron bunch.

ACKNOWLEDGMENTS

The authors are grateful to Prof. A. P. Ulyanenko for valuable discussions and support during the project.

-
- [1] V. G. Baryshevsky, I. D. Feranchuk, and A. P. Ulyanenko, *Parametric X-Ray Radiation in Crystals: Theory, Experiment and Applications (Springer Tracts in Modern Physics)* (Springer, 2006).
- [2] J. Hyun, M. Satoh, M. Yoshida, T. Sakai, Y. Hayakawa, T. Tanaka, K. Hayakawa, I. Sato, and K. Endo, *Phys. Rev. Accel. Beams* **21**, 014701 (2018).
- [3] Y. Hayakawa, I. Sato, K. Hayakawa, T. Tanaka, A. Mori, T. Kuwada, T. Sakai, K. Nogami, K. Nakao, and T. Sakae, *Nuclear Instruments and Methods in Physics Research Section B: Beam Interactions with Materials and Atoms* **252**, 102 (2006), relativistic Channeling and Coherent Phenomena in Strong Fields.
- [4] W. Lauth, H. Backe, O. Kettig, P. Kunz, A. Sharafutdinov, and T. Weber, *The European Physical Journal A - Hadrons and Nuclei* **28**, 185 (2006).
- [5] K. H. Brenzinger, C. Herberg, B. Limburg, H. Backe, S. Dambach, H. Euteneuer, F. Hagenbuck, H. Hartmann, K. Johann, K. H. Kaiser, O. Kettig, G. Knies, G. Kube, W. Lauth, H. Schöpe, and T. Walcher, *Zeitschrift für Physik A Hadrons and Nuclei* **358**, 107 (1997).
- [6] K.-H. Brenzinger, B. Limburg, H. Backe, S. Dambach, H. Euteneuer, F. Hagenbuck, C. Herberg, K. H. Kaiser, O. Kettig, G. Kube, W. Lauth, H. Schöpe, and T. Walcher, *Phys. Rev. Lett.* **79**, 2462 (1997).
- [7] P. Rullhusen, X. Artru, and P. Dhez, *Novel Radiation Sources Using Relativistic Electrons: From Infrared to X-rays*, Series in Mathematical Biology and Medicine (World Scientific, 1998).
- [8] O. D. Skoromnik, I. D. Feranchuk, J. Evers, and C. H. Keitel, *Phys. Rev. Accel. Beams* **25**, 040704 (2022).
- [9] V. Baryshevsky and I. Feranchuk, *Physics Letters A* **102**, 141 (1984).
- [10] A. Gover, R. Ianculescu, A. Friedman, C. Emma, N. Sudar, P. Musumeci, and C. Pellegrini, *Rev. Mod. Phys.* **91**, 035003 (2019).
- [11] O. D. Skoromnik, V. G. Baryshevsky, A. P. Ulyanenko, and I. D. Feranchuk, *Nuclear Instruments and Methods in Physics Research Section B: Beam Interactions with Materials and Atoms* **412**, 86 (2017).
- [12] A. Akhiezer and V. Berestetskii, *Quantum electrodynamics*, Interscience monographs and texts in physics and astronomy (Interscience, 1965).
- [13] M. L. Ter-Mikaelian, *High-energy electromagnetic processes in condensed media*, 29 (John Wiley & Sons, 1972).
- [14] L. D. Landau and E. M. Lifshitz, *The Classical Theory of Fields*, Course of theoretical physics (Butterworth-Heinemann, 1975).

- [15] Here and through the manuscript we use natural units with $\hbar = c = 1$.
- [16] Z. Huang and K.-J. Kim, *Phys. Rev. ST Accel. Beams* **10**, 034801 (2007).
- [17] J. Feldhaus, M. Krikunova, M. Meyer, T. Möller, R. Moshhammer, A. Rudenko, T. Tschentscher, and J. Ullrich, *Journal of Physics B: Atomic, Molecular and Optical Physics* **46**, 164002 (2013).
- [18] E. Janke and E. Emde, *Tafeln Hoherer Funktionen* (1960).
- [19] A. Authier, *Dynamical Theory of X-ray Diffraction*, International Union of Crystallography monographs on crystallography (Oxford University Press, 2001).
- [20] M. Born and E. Wolf, *Principles of Optics: Electromagnetic Theory of Propagation, Interference and Diffraction of Light* (Elsevier Science, 2013).
- [21] O. D. Skoromnik, I. D. Feranchuk, and D. V. Lu, *Nuclear Instruments and Methods in Physics Research Section B: Beam Interactions with Materials and Atoms* **444**, 125 (2019).
- [22] A. Benediktovich, I. Feranchuk, and A. Ulyanenkov, *Theoretical Concepts of X-Ray Nanoscale Analysis: Theory and Applications*, Springer Series in Materials Science (Springer Berlin Heidelberg, 2013).
- [23] I. Feranchuk and A. Ivashin, *J. Phys. France* **46**, 1981 (1985).
- [24] S. A. Stepanov, “X-ray dynamical diffraction web server,” <http://x-server.gmca.aps.anl.gov/>, accessed: 19-06-2022.